A numerical study of universality and self-similarity in the Forced Logistic Map*

Pau Rabassa[1], Angel Jorba[2], and Joan Carles Tatjer[2]

[1]Johann Bernoulli Institute for Mathematics and Computer Science,
University of Groningen, Groningen, The Netherlands
E-mail: paurabassa@gmail.com

[2]Departament de Matemàtica Aplicada i Anàlisi,
Universitat de Barcelona, Barcelona, Spain
E-mails: angel@maia.ub.edu, jcarles@maia.ub.es

April 16, 2012

Abstract

We explore different two parametric families of quasi-periodically Forced Logistic Maps looking for universality and self-similarity properties. In the bifurcation diagram of the one-dimensional Logistic Map it is well known that there exist parameter values s_n where the 2^n-periodic orbit is superattracting. Moreover, these parameter values lay between the parameters corresponding to two consecutive period doublings. In the quasi-periodically Forced Logistic Maps, these points are replaced by invariant curves, that undergo a (finite) sequence of period doublings.

In this work we study numerically the presence of self-similarities in the bifurcation diagram of the invariant curves of these quasi-periodically Forced Logistic Maps. Our computations show a remarkable self-similarity for some of these families. We also show that this self-similarity cannot be extended to any quasi-periodic perturbation of the Logistic map.

1 Introduction

Universality and self-similarity properties of uniparametric families of unimodal maps are a well known phenomenon, being one of the paradigmatic examples the Logistic Map $l_\alpha(x) = \alpha x(1-x)$. Given a typical one parametric family of unimodal maps $\{l_\alpha\}_{\alpha \in I}$ one observes numerically that there exists a sequence of parameter values $\{d_n\}_{n \in \mathbb{N}} \subset I$ such that the attracting periodic orbit of the map undergoes a period doubling bifurcation. Between one period doubling and the next there exists a parameter value s_n, for which the critical point of l_{s_n} is a periodic orbit with period 2^n. Moreover,

$$\lim_{n\to\infty} \frac{d_n - d_{n-1}}{d_{n+1} - d_n} = \lim_{n\to\infty} \frac{s_n - s_{n-1}}{s_{n+1} - s_n} = \delta = \ 4.66920\ldots \tag{1}$$

The convergence to this limit $\boldsymbol{\delta}$ (the so-called Feigenbaum constant) indicates a self-similarity on the parameter space of the family. On the other hand, the constant $\boldsymbol{\delta}$ is universal, in the sense that one obtains the same ratio $\boldsymbol{\delta}$ for any family of unimodal maps with a quadratic turning point having a cascade of period doubling bifurcations ([5]). In this paper we explore the same kind of phenomenon when the one dimensional map is quasi-periodically forced. We will see that universality and self-similarity do manifest, but in different manners. Moreover, we show that they occur in a more "restrictive" class of maps, in the sense that the quasi-periodic forcing has to have a very particular form.

A **quasi-periodically forced one dimensional map** is a map of the form

$$
\begin{array}{cccc}
F : & \mathbb{T} \times \mathbb{R} & \to & \mathbb{T} \times \mathbb{R} \\
& \begin{pmatrix} \theta \\ x \end{pmatrix} & \mapsto & \begin{pmatrix} \theta + \omega \\ f(\theta, x) \end{pmatrix}
\end{array}
\tag{2}
$$

where $f \in C^r(\mathbb{T} \times \mathbb{R}, \mathbb{R})$ with $r \geq 1$ and $\omega \in \mathbb{T} \setminus \mathbb{Q}$. A quasi-periodically forced map determines a dynamical system on the cylinder, explicitly defined as

$$
\left.
\begin{aligned}
\bar{\theta} &= \theta + \omega, \\
\bar{x} &= f(\theta, x).
\end{aligned}
\right\}
\tag{3}
$$

Given a continuous function $u : \mathbb{T} \to \mathbb{R}$ we will say that u is an **invariant curve** of (3) if, and only if,

$$
u(\theta + \omega) = f(\theta, u(\theta)), \quad \forall \theta \in \mathbb{T}.
$$

The value ω is known as the **rotation number** of the curve. An equivalent way to define an invariant curve is to require the set $\{(\theta, x) \in \mathbb{T} \times \mathbb{R} \mid x = u(\theta)\}$ to be invariant by F, where F is the function defined by (2). On the other hand, note that F^n is also a quasi-periodically forced map.

Given a function $u : \mathbb{T} \to \mathbb{R}$, we will say that u is a n-**periodic invariant curve** of F if u is invariant by F^n (and there is no smaller n satisfying such condition).

Given $x = u_0(\theta)$ an invariant curve of (3) of class C^r ($r \geq 1$), its linearized normal behaviour is described by the following linear skew product:

$$
\left.
\begin{aligned}
\bar{\theta} &= \theta + \omega, \\
\bar{x} &= a(\theta)x,
\end{aligned}
\right\}
\tag{4}
$$

where $a(\theta) = D_x f(\theta, u_0(\theta))$ is of class C^{r-1}, $x \in \mathbb{R}$ and $\theta \in \mathbb{T}$.

A linear skew product like (4) is called **reducible** if, and only if, there exists a change of variable $x = c(\theta)y$, continuous with respect to θ, such that (4) becomes

$$
\left.
\begin{aligned}
\bar{\theta} &= \theta + \omega, \\
\bar{y} &= by,
\end{aligned}
\right\}
$$

where b does not depend on θ. The constant b is called the **multiplier** of the reduced system. An invariant curve is called **reducible** if its linearized normal behaviour (4) is reducible. An n-periodic invariant curve is reducible if it is reducible for F^n.

In the case that $a(\cdot)$ is a C^∞ function and ω is Diophantine, the skew product (4) is reducible if, and only if, $a(\cdot)$ has no zeros. Due to this property, the reducibility loss can be characterized as a codimension one bifurcation.

Let us consider a one-parametric family of linear skew-products

$$\begin{aligned} \bar{\theta} &= \theta + \omega, \\ \bar{x} &= a(\theta, \mu)x, \end{aligned} \Bigg\} \tag{5}$$

where ω is Diophantine, μ belongs to an open set of $\mathbb{R}$ and a is a C^∞ function of θ and μ. We will say that the system (5) undergoes a **reducibility loss bifurcation** at μ_0 if

1. $a(\cdot, \mu)$ has no zeros for $\mu < \mu_0$,

2. $a(\cdot, \mu)$ has a double zero at θ_0 for $\mu = \mu_0$,

3. $\frac{d}{d\mu}a(\theta_0, \mu_0) \neq 0$.

On the other hand, consider a system like (3) with f a C^∞ function, which depends (smoothly) on a one dimensional parameter μ (we denote this dependence as $f = f_\mu$), having an invariant curve $u = u_\mu$. We will say that **the invariant curve undergoes a reducibility loss bifurcation** if the family of linear skew-products (5), where $a(\theta, \mu) = D_x f_\mu(\theta, u_\mu(\theta))$, undergoes a reducibility loss bifurcation. For more details see Section 2.1 in [12] or Section 3 in [13].

Given a map like (4) we have that, due to the rigid rotation in the periodic component, one of its Lyapunov exponents is equal to zero (see [1]). Then the definition of the Lyapunov exponent can be suited to the case of linear skew-products as follows.

If $\theta \in \mathbb{T}$, we define the **Lyapunov exponent** of (4) at θ as

$$\lambda(\theta) = \limsup_{n \to \infty} \frac{1}{n} \ln \left| \prod_{j=0}^{n-1} a(\theta + j\omega) \right|. \tag{6}$$

We also define the **Lyapunov exponent of the skew product** (4) as

$$\Lambda = \int_0^1 \ln |a(\theta)| d\theta.$$

If Λ is finite then, applying the Birkhoff Ergodic Theorem we have that the $\limsup$ in (6) is in fact a limit and $\lambda(\theta) = \Lambda$ for Lebesgue a.e. $\theta \in \mathbb{T}$. If $a(\theta)$ never vanishes, the $\limsup$ in (6) is again a limit and coincides with Λ, but now for all $\theta \in \mathbb{T}$.

Quasi-periodically forced one dimensional maps have been extensively studied ([8, 9, 15, 10, 6, 13, 3, 7]) with a focus on the existence of strange non-chaotic attractors.

The kind of maps that we consider here are like (3), where f is given by an unimodal one dimensional map plus a small perturbation which depends on both variables x and θ. The paradigmatic example in our case of study is the Forced Logistic Map, which is defined as

$$\begin{aligned} \bar{\theta} &= \theta + \omega, \\ \bar{x} &= \alpha x(1 - x)(1 + \varepsilon \cos(2\pi\theta)), \end{aligned} \Bigg\} \tag{7}$$

where (α, ε) are parameters and ω is a fixed irrational number. This family has interest not only for phenomena related with the existence of strange non-chaotic attractors ([9, 15, 6]) but also as a model for the truncation of period doubling bifurcation cascade ([14, 12]). The term "truncation of the period doubling bifurcation cascade" refers to the fact that, for fixed ε and growing α, the attracting set of the map undergoes only a finite number of period doubling
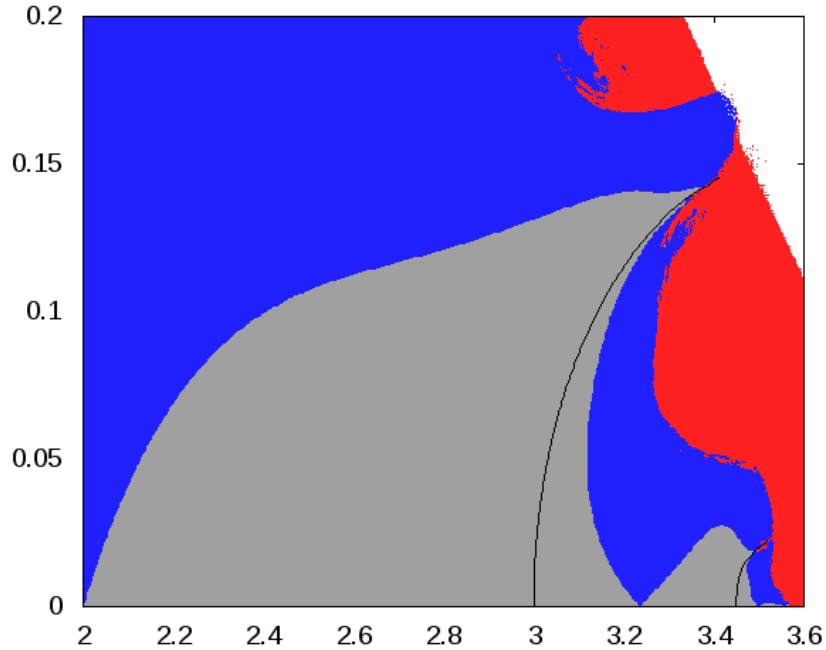
3

Figure 1: Diagram of the parameter space of the map (7) for $\omega = \frac{\sqrt{5}-1}{2}$. The axes correspond to the parameters α (horizontal) and ε (vertical). The black lines represent the period doubling bifurcations from period one to two (left) and two to four (right). The colour coding is the following: Black means "invariant curve with zero Lyapunov exponent", red means "chaotic attractor", blue means "non-chaotic non-reducible attractor", grey means "non-chaotic reducible attractor" and white refers to "no attractor (divergence to $-\infty$)".

bifurcations before exhibiting a chaotic behaviour. This differs from the one dimensional case, where there are infinitely many period doubling bifurcations before chaos.

In [12] we studied the truncation of the period doubling cascade for the map (7). We observed that the reducibility of the invariant curves plays a crucial role. We note that, in this example and for $|\varepsilon| < 1$, $D_x f(\theta, x)$ is zero if and only $x = \frac{1}{2}$. Hence, if $|\varepsilon| < 1$, an invariant curve is reducible if and only if it does not intersect the line $x = \frac{1}{2}$. We computed bifurcation diagrams in terms of the dynamics of the attracting set, taking into account different properties, as the Lyapunov exponent and, in the case of having a periodic invariant curve, its period and reducibility. One of these bifurcation diagrams is reproduced in Figure 1.

Let d_n be the value of the parameter α where the attracting periodic orbit of the one dimensional map doubles from period 2^n to period 2^{n+1}. Figure 1 shows that from every parameter $(\alpha, \varepsilon) = (d_n, 0)$ of the map (7), a period doubling bifurcation curve of invariant curves is born. Let s_n be the parameter value where the critical point of the (non-forced) one dimensional family is periodic with period 2^n. Figure 1 also shows that from every parameter value $(\alpha, \varepsilon) = (s_n, 0)$ two curves of reducibility loss are born. The left curve (namely, S_n^-) corresponds to a passage from a reducible to non-reducible 2^n-periodic invariant curve, while the right curve (S_n^+) corresponds to a passage from non-reducible to reducible of the same 2^n-periodic invariant curve. In [17] we prove, under suitable hypotheses, that these curves exist. In Figure 1 we can observe that the period doubling bifurcation curve born at $(d_n, 0)$ is between the right reducibility loss bifurcation curve born at $(s_n, 0)$ and the left reducibility loss bifurcation curve born at $(s_{n+1}, 0)$.

4

In this paper we study, numerically, the extension of this self-similarity to the quasi-periodically Forced Logistic Map. To this end, we approximate numerically the reducibility loss bifurcations curves S_n^- and S_n^+ near $(\alpha, \varepsilon) = (s_n, 0)$. As we will see, there are self-similarities between these curves.

2 The curves of reducibility loss

In this section we focus on the reducibility loss curves $S_n^\pm$ born at the points $(\alpha, \varepsilon) = (s_n, 0)$, for ε small. To start, let us assume that each of these curves is the graph of a function depending on ε (this assumption is discussed in [17]). In other words, there exist a neighbourhood U_n of s_n, an interval $I = [0, \rho)$ and functions $\alpha_n^\pm : I \to \mathbb{R}$ such that $S_n^\pm \cap U_n = \{(\alpha_n^\pm(\varepsilon), \varepsilon) \mid \varepsilon \in I\}$.

To compute values of the curve $(\alpha_n^\pm(\varepsilon), \varepsilon)$ we have used the following procedure. First, the 2^n periodic invariant curve of (7) is written as a truncated Fourier series and then the invariance condition gives an equation (that also depends on the parameters α and ε) for these coefficients (see [4] or [11] for more details). This equation is then supplemented by a second equation that is the condition of reducibility loss bifurcation of the curve (in this case, this is to ask that the curve has a tangency with the line $x = \frac{1}{2}$). The role of this condition is to impose a relation between both parameters which defines the curves $S_n^\pm$ we are looking for. Finally, a standard continuation procedure on these two equations allows to compute the desired curves. A similar scheme was used in [12] to compute the curve of zero Lyapunov exponent.

Assume that the functions $\alpha_n^\pm(\varepsilon)$ are written at first order as

$$\alpha_n^\pm(\varepsilon) = s_n + \widetilde{\alpha}_n^\pm \varepsilon + O(\varepsilon^2).$$

That is, $\widetilde{\alpha}_n^\pm$ denotes the derivative of $\alpha_n^\pm(\varepsilon)$ at $\varepsilon = 0$. To obtain a numerical approximation of the values $\widetilde{\alpha}_n^\pm$ we have used the previous procedure to compute points $(\alpha_n^\pm(\varepsilon), \varepsilon) \in S_n^\pm$ for $\varepsilon = 2^{-k} h_n$ for $k = 1, 2, ..., M$, being h_n a prescribed small value (the larger the n, the smaller h_n). Then, we can use a forward difference to estimate $\widetilde{\alpha}_n^\pm$:

$$\widetilde{\alpha}_n^\pm \approx \frac{\alpha_n^\pm(2^{-k} h_n) - \alpha_n^\pm(0)}{2^{-k} h_n}.$$

To improve the accuracy, we have done three steps of Richardson extrapolation. To estimate the accuracy of the results, we have repeated this same extrapolation but halving the value of h_n. All these computations have been done with quadruple precision, using the library [2].

Lemma 1 *Let us consider a map of the form,*

$$\left. \begin{array}{rcl} \bar{\theta} & = & \theta + \omega, \\ \bar{x} & = & h(x, \theta, \alpha, \varepsilon), \end{array} \right\}$$

satisfying the symmetry $h(x, \theta, \alpha, \varepsilon) = h(x, \theta + \frac{1}{2}, \alpha, -\varepsilon)$. *If there is a reducibility loss bifurcation curve* $(\varepsilon, \alpha(\varepsilon))$, *then* $(-\varepsilon, \alpha(\varepsilon))$ *is also a reducibility loss bifurcation curve.*

The proof is obvious noting that the map is conjugated (by $\theta \mapsto \theta + \frac{1}{2}$) to the same map but replacing ε by $-\varepsilon$.

Note that Lemma 1 implies, in our case, that $\widetilde{\alpha}_n^- = -\widetilde{\alpha}_n^+$. As a test of our calculations, we have computed both values $\widetilde{\alpha}_n^\pm$, and in all the cases the values obtained satisfy $\widetilde{\alpha}_n^- = -\widetilde{\alpha}_n^+$ (within

n	$\widetilde{\alpha}_n(\omega)$	$\widetilde{\alpha}_n(\omega)/\widetilde{\alpha}_{n-1}(\omega)$	ϵ_a
0	−2.0000000000e+00	– – –	3.0e−15
1	−5.8329149229e+00	2.9164574614e+00	1.5e−14
2	−8.4942599432e+00	1.4562633015e+00	8.4e−13
3	−1.6351279467e+01	1.9249798777e+00	7.4e−15
4	−1.1252460775e+01	6.8817004793e−01	3.0e−14
5	−1.2243326651e+01	1.0880577054e+00	1.6e−13
6	−1.8079693906e+01	1.4766978307e+00	1.6e−11
7	−3.4735234067e+01	1.9212291009e+00	2.0e−12
8	−2.9583312211e+01	8.5168023205e−01	2.1e−12
9	−4.1569457725e+01	1.4051657715e+00	4.2e−10
10	−7.8965495522e+01	1.8996036957e+00	9.1e−11
11	−7.4500733455e+01	9.4345932945e−01	8.1e−10

Table 1: Approximate values of $\widetilde{\alpha}_n(\omega)$ for the map (7) for $\omega = \frac{\sqrt{5}-1}{2}$.

n	$\widetilde{\alpha}_n(\omega)$	$\widetilde{\alpha}_n(\omega)/\widetilde{\alpha}_{n-1}(\omega)$	ϵ_a
0	−2.0000000000e+00	– – –	4.1e−16
1	−4.7793787548e+00	2.3896893774e+00	9.2e−14
2	−9.9177338359e+00	2.0751094117e+00	8.0e−16
3	−6.9333908531e+00	6.9909023249e−01	4.3e−15
4	−7.5678156188e+00	1.0915028129e+00	2.4e−14
5	−1.1183261803e+01	1.4777397292e+00	2.3e−12
6	−2.1488744556e+01	1.9215095679e+00	3.0e−13
7	−1.8302110429e+01	8.5170682641e−01	3.1e−13
8	−2.5717669657e+01	1.4051750893e+00	6.1e−11
9	−4.8853450105e+01	1.8996064090e+00	2.6e−11
10	−4.6091257360e+01	9.4345961772e−01	1.2e−10
11	−7.1498516059e+01	1.5512381339e+00	4.1e−09

Table 2: Approximate values of $\widetilde{\alpha}_n(\omega)$ for the map (7) for $\omega = 2\frac{\sqrt{5}-1}{2}$.

the accuracy of the computations). Hence, in what follows we only focus on the values $\widetilde{\alpha}_n^-$. To simplify the notation, from now on we will refer to $\widetilde{\alpha}_n^-$ as $\widetilde{\alpha}_n$.

The values of $\widetilde{\alpha}_n$ depend on ω, the rotation number of the system. Hence, from now on, we write $\widetilde{\alpha}_n = \widetilde{\alpha}_n(\omega)$. The estimated values of $\widetilde{\alpha}_n(\omega)$ for the family (7) when $\omega = \frac{\sqrt{5}-1}{2}$ are shown in Table 1. We have included the ratios $\widetilde{\alpha}_n(\omega)/\widetilde{\alpha}_{n-1}(\omega)$ in the third column of the table. The value ϵ_a in the fourth column corresponds to the estimated absolute error of the value of $\widetilde{\alpha}_n$. In Tables 2 and 3 we have included the same values for $\omega = 2\frac{\sqrt{5}-1}{2}$ and $\omega = 4\frac{\sqrt{5}-1}{2}$.

A remarkable fact is that the ratios $\widetilde{\alpha}_n(\omega)/\widetilde{\alpha}_{n-1}(\omega)$ on the third column of Table 1 are approximately the same values on the third column of Table 2, but shifted on the index value n by one position. In fact, the bigger is n the closer are the values. The same phenomenon can be observed in Tables 2 and 3. We can also observe in Tables 1, 2 and 3 that the ratios $\widetilde{\alpha}_n(\omega)/\widetilde{\alpha}_{n-1}(\omega)$ do not converge to a constant value. However, in the following sections we will obtain some self-similarity properties of this family.

n	$\widetilde{\alpha}_n(\omega)$	$\widetilde{\alpha}_n(\omega)/\widetilde{\alpha}_{n-1}(\omega)$	ϵ_a
0	-2.0000000000e+00	- - -	5.3e-15
1	-6.1135714539e+00	3.0567857269e+00	4.0e-17
2	-4.6432689399e+00	7.5950186809e-01	8.8e-16
3	-5.1662366620e+00	1.1126292121e+00	5.4e-15
4	-7.6637702641e+00	1.4834338350e+00	5.2e-13
5	-1.4738755184e+01	1.9231728870e+00	6.7e-14
6	-1.2555429245e+01	8.5186497017e-01	6.9e-14
7	-1.7643286059e+01	1.4052316105e+00	1.3e-11
8	-3.3515585777e+01	1.8996226477e+00	5.8e-12
9	-3.1620659727e+01	9.4346134772e-01	2.6e-11
10	-4.9051192417e+01	1.5512387420e+00	9.0e-10
11	-9.2911119039e+01	1.8941663691e+00	5.6e-12

Table 3: Approximate values of $\widetilde{\alpha}_n(\omega)$ for the map (7) for $\omega = 4\frac{\sqrt{5}-1}{2}$.

2.1 Universality of the ratio sequence

Let F be a quasi-periodic forced map like (2) where f is a C^r map and ω an irrational number. We suppose that this map depends on two parameters α, ε such that, if $\varepsilon = 0$ then f does not depend on θ and it has a cascade of period doubling bifurcations with respect to α. Moreover we assume, for ε small, that the reducibility-loss bifurcation curves are well defined as differentiable functions with respect to ε. In what follows, we will write explicitly the dependence on f of the slopes of these curves as $\widetilde{\alpha}_n(\omega, f)$. Now we can resume the discussion on the phenomenon observed on Tables 1, 2 and 3. Our numerical computations suggest that, for large n,

$$\frac{\widetilde{\alpha}_n(\omega, f)}{\widetilde{\alpha}_{n-1}(\omega, f)} \approx \frac{\widetilde{\alpha}_{n-1}(2\omega, f)}{\widetilde{\alpha}_{n-2}(2\omega, f)}. \tag{8}$$

Consider two different values ω_0 and ω_1 such that $2\omega_0 = 2\omega_1 (\mathrm{mod}\, 1)$. If (8) is true, then $\widetilde{\alpha}_n(\omega_0, f)/\widetilde{\alpha}_{n-1}(\omega_0, f) \approx \widetilde{\alpha}_n(\omega_1, f)/\widetilde{\alpha}_{n-1}(\omega_1, f)$ if n is large. To check it, in Table 4 we have recomputed the same values as in Table 1 but this time for $\omega = \frac{\sqrt{5}}{2}$ (and f the function associated to the map (7) as before).

If F denotes a quasi-periodically forced map (2), let F^2 be the map composed with itself. Concretely, the map F^2 can be written as $F^2(\theta, x) = (\theta + 2\omega, f(\theta + \omega, f(\theta, x)))$. To simplify the notation, let us denote by f^2 the map defined as $f^2(\theta, x) := f(\theta + \omega, f(\theta, x))$. Moreover we have that the 2^k periodic curves of F are 2^{k-1} periodic curves of the map F^2, therefore $\widetilde{\alpha}_n(\omega, f) = \widetilde{\alpha}_{n-1}(2\omega, f^2)$. Hence, for n large, the relation given by (8) can be rewritten as

$$\frac{\widetilde{\alpha}_n(2\omega, f^2)}{\widetilde{\alpha}_{n-1}(2\omega, f^2)} \approx \frac{\widetilde{\alpha}_n(2\omega, f)}{\widetilde{\alpha}_{n-1}(2\omega, f)}. \tag{9}$$

Now we have that the relation given by (8) can be explained as a consequence of a much more general phenomenon. We believe that the sequence $\frac{\widetilde{\alpha}_n(\omega, f)}{\widetilde{\alpha}_{n-1}(\omega, f)}$ is (asymptotically) **universal**, in the sense that it does not depend on the map f. This would imply (9) and consequently (8).

To check the universality of the sequence, we consider the following map,

$$\left. \begin{array}{rcl} \bar{\theta} & = & \theta + \omega, \\ \bar{x} & = & \alpha x(1 - x) + \varepsilon \cos(2\pi\theta). \end{array} \right\} \tag{10}$$

n	$\widetilde{\alpha}_n(\omega)$	$\widetilde{\alpha}_n(\omega)/\widetilde{\alpha}_{n-1}(\omega)$	ϵ_a
0	-2.0000000000e+00	- - -	5.3e-17
1	-3.7459592187e+00	1.8729796094e+00	3.6e-15
2	-6.1798012892e+00	1.6497246575e+00	2.4e-13
3	-1.2170152952e+01	1.9693437350e+00	2.1e-15
4	-8.4095313813e+00	6.9099635922e-01	9.5e-15
5	-9.1576001570e+00	1.0889548706e+00	5.2e-14
6	-1.3525371011e+01	1.4769558377e+00	5.0e-12
7	-2.5986306241e+01	1.9213008072e+00	6.5e-13
8	-2.2132200091e+01	8.5168703416e-01	6.6e-13
9	-3.1099463199e+01	1.4051681745e+00	1.3e-10
10	-5.9076676864e+01	1.8996043914e+00	5.6e-11
11	-5.5736446311e+01	9.4345940345e-01	2.5e-10

Table 4: Approximate values of $\widetilde{\alpha}_n(\omega)$ for the map (7) for $\omega = \frac{\sqrt{5}}{2}$.

n	$\widetilde{\alpha}_n(\omega)$	$\widetilde{\alpha}_n(\omega)/\widetilde{\alpha}_{n-1}(\omega)$	ϵ_a
0	-4.0000000000e+00	- - -	2.7e-14
1	-8.1607837043e+00	2.0401959261e+00	5.1e-14
2	-1.1166652707e+01	1.3683309241e+00	2.4e-12
3	-2.1221554117e+01	1.9004400578e+00	2.1e-14
4	-1.4564213015e+01	6.8629342294e-01	8.6e-14
5	-1.5837452605e+01	1.0874224778e+00	4.6e-13
6	-2.3384207858e+01	1.4765132021e+00	4.5e-11
7	-4.4925217655e+01	1.9211776567e+00	5.8e-12
8	-3.8261700375e+01	8.5167534788e-01	5.9e-12
9	-5.3763965691e+01	1.4051640456e+00	1.1e-09
10	-1.0213020106e+02	1.8996031960e+00	1.1e-10
11	-9.6355685578e+01	9.4345927630e-01	2.3e-09

Table 5: Approximate values of $\widetilde{\alpha}_n$ for the map (10) for $\omega = \frac{\sqrt{5}-1}{2}$.

n	$\widetilde{\alpha}_n(\omega)$	$\widetilde{\alpha}_n(\omega)/\widetilde{\alpha}_{n-1}(\omega)$	ϵ_a
0	-4.0000000000e+00	- - -	3.8e-15
1	-6.2417012728e+00	1.5604253182e+00	2.4e-13
2	-1.2036825830e+01	1.9284527253e+00	2.1e-15
3	-8.2891818940e+00	6.8865180997e-01	9.0e-15
4	-9.0187641307e+00	1.0880161934e+00	4.9e-14
5	-1.3318271659e+01	1.4767291245e+00	4.7e-12
6	-2.5587438370e+01	1.9212281462e+00	6.1e-13
7	-2.1792312360e+01	8.5168011135e-01	6.2e-13
8	-3.0621808757e+01	1.4051656497e+00	1.2e-10
9	-5.8169300479e+01	1.8996036760e+00	5.2e-11
10	-5.4880369083e+01	9.4345932701e-01	2.3e-10
11	-8.5132515708e+01	1.5512380316e+00	8.2e-09

Table 6: Approximate values of $\widetilde{\alpha}_n$ for the map (10) for $\omega = 2\frac{\sqrt{5}-1}{2}$.

This map is like (7) but with an additive forcing instead of a multiplicative one. In the literature, sometimes (7) is referred as the Driven Logistic Map and (10) is referred as the Forced Logistic Map. In this paper we consider both as two different versions of the Forced Logistic Map.

Note that both maps are in the class of quasi-periodically forced one dimensional unimodal maps, with a quasi-periodic forcing of the type $h(x)\cos(2\pi\theta)$, where h is a function of one variable. This is certainly a very restrictive class of maps. In Section 4 we explore what happens when the quasi-periodic forcing is not of this form.

We have computed the slopes $\widetilde{\alpha}_n(\omega)$, the associated ratios $\widetilde{\alpha}_n(\omega)/\widetilde{\alpha}_{n-1}(\omega)$ and the estimation of their accuracy for the family (10) as it was done for the family (7). The results are shown in Table 5 for $\omega = \frac{\sqrt{5}-1}{2}$ and in Table 6 for $\omega = 2\frac{\sqrt{5}-1}{2}$.

Now we can compare the sequences $\widetilde{\alpha}_n(\omega_0)/\widetilde{\alpha}_{n-1}(\omega_0)$ in Tables 1 and 2, with the ones in Tables 5 and 6 respectively. Again we can observe that both sequences have an equivalent asymptotic behaviour for equal values of ω. This agrees with the conjectured universal behaviour.

3 Self-similarity of the bifurcation diagram

Given a one dimensional map in the interval $g : I \to I$, its (doubling) renormalization is defined as $\mathcal{R}(f) = A^{-1} \circ g \circ g \circ A$ with A an affine transformation. Note that the self-similarity (1) in the bifurcation diagram of the Logistic Map can also be seen in the following way. If s^* is the limit of the sequence of parameter values s_n, then $s_n - s^* \approx \boldsymbol{\delta}(s_{n+1} - s^*)$. In terms of the parameter space this means that the affine map $L(\alpha) = \boldsymbol{\delta}(\alpha - s^*) + s^*$ sends (approximately) the point s_n to s_{n-1}. Given a q.p. forced map like (2), one might try to define a renormalization for these kind of maps. The most simple choice would be to define its (doubling) renormalization also as $\mathcal{T}(F) = A^{-1} \circ F \circ F \circ A$, with A a suitable affine map. If the map F has rotation number ω, its (doubling) renormalization will have rotation number 2ω. This is due to the composition of F with itself when we define its renormalization.

The reducibility loss curves $S_n^{\pm}$ in the parameter space of the map (7) depend on the rotation number (i.e. $S_n^{\pm} = S_n^{\pm}(\omega)$). We can look for self-similarity of the parameter space, but taking into account the "doubling" of the rotation number. In other words, we look for an affine relationship between the slopes of the curves $S_n^{\pm}$ around s_n for ω_0 and the slope of the same curves for $2\omega_0$. That is, we look for an affine map of the kind

$$L\begin{pmatrix} \alpha \\ \varepsilon \end{pmatrix} = \begin{pmatrix} \delta_0 & 0 \\ 0 & \delta_1 \end{pmatrix} \begin{pmatrix} \alpha - s^* \\ \varepsilon \end{pmatrix} + \begin{pmatrix} s^* \\ 0 \end{pmatrix}, \tag{11}$$

such that it maps the curves $S_n^-(2\omega)$ to $S_{n-1}^-(\omega)$ (and respectively $S_n^+(2\omega)$ to $S_{n-1}^+(\omega)$). If we impose these conditions to the local parameterization (around s_n) of the curves considered above then we get

$$\begin{pmatrix} s_{n-1} + \widetilde{\alpha}_{n-1}(2\omega)t + o(t) \\ t \end{pmatrix} = \begin{pmatrix} \delta_0 & 0 \\ 0 & \delta_1 \end{pmatrix} \begin{pmatrix} s_n + \widetilde{\alpha}_n(\omega)s + o(s) - s^* \\ s \end{pmatrix} + \begin{pmatrix} s^* \\ 0 \end{pmatrix},$$

for any t and s. Then, replacing $s = t/\delta_1$ in the first coordinate and equating terms in the order of t, we obtain

$$s_{n-1} = \delta_0 s_n + (1 - \delta_0)s^*$$
$$\widetilde{\alpha}_{n-1}(2\omega) = \frac{\delta_0}{\delta_1}\widetilde{\alpha}_n(\omega).$$
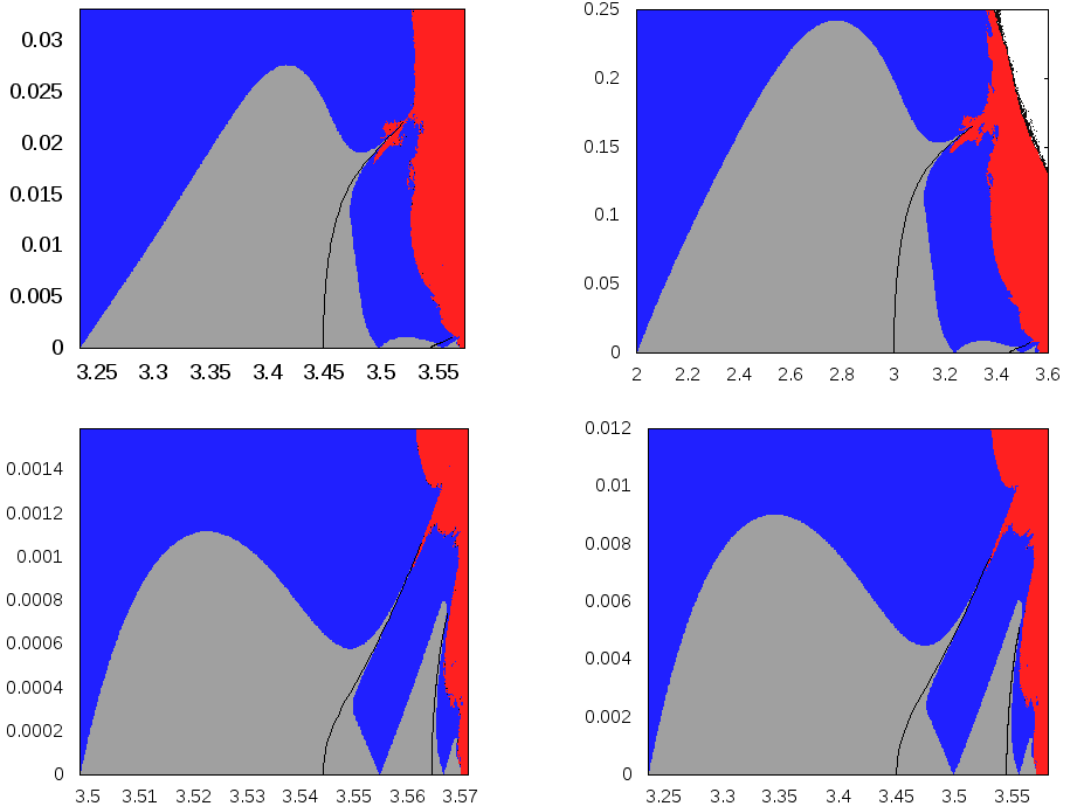
<div align="center">9</div>

Figure 2: Diagram of the parameter space of the map (7) for $\omega = \frac{\sqrt{5}-1}{2}$ on the left hand side and for $\omega = \sqrt{5} - 1$ on the right. Color codes are the same as in Figure 1.

Using these two equations we have that the value δ_1 can be estimated as $\delta_1 \approx \delta_0 \frac{\widetilde{\alpha}_n(\omega)}{\widetilde{\alpha}_{n-1}(2\omega)}$. For δ_0 we recover the estimation $\delta_0 \approx \frac{s_n - s_{n-1}}{s_{n-1} - s_{n-2}}$, which converges to the Feigenbaum constant $\boldsymbol{\delta}$. Therefore we replace δ_0 by $\boldsymbol{\delta}$ in the estimation of δ_1, obtaining $\delta_1 \approx \boldsymbol{\delta} \frac{\widetilde{\alpha}_n(\omega)}{\widetilde{\alpha}_{n-1}(2\omega)}$.

In Table 7 we have estimations of these values for the family (7) for $\omega = \frac{\sqrt{5}-1}{2}$ (left) and $\omega = \sqrt{5} - 1$ (right). In Table 8 we have the same estimation for the family (10) and $\omega = \frac{\sqrt{5}-1}{2}$. In all the cases the sequence seems to converge to a concrete value. This convergence means that there exists an affine relation between the reducibility loss bifurcation curves $S_n^\pm(\omega)$ and $S_{n-1}^\pm(2\omega)$ around the superstable periodic orbits of the uncoupled map. Note that the limit constants obtained in each of these three cases are different one to each other. This indicates that the renormalization factor depends both on the value of ω taken and the family of maps considered. Therefore the renormalization factor δ_1 is not universal.

These evidences of self-similarity are only valid for infinitely small values of the coupling parameter ε. If the self-similarity between families extends to larger values of ε, the bifurcation diagram of the map (7) in a box $I_1 \times I_2$ of the parameters space for a prescribed $\omega = \omega_0$ should be approximately the same as the diagram in the box $L(I_1 \times I_2)$ for $\omega = 2\omega_0$, where L is the affine map (11).

In Figure 2 we have a bifurcation diagram of the map (7) analog to the one displayed in Figure 1. The scale of the boxes has been selected such that the one in the left is the image of the one

10

n	$\delta_{1,n}(\omega_0)$	$\delta_{1,n} - \delta_{1,n-1}$	$\delta_{1,n}(\omega_0)$	$\delta_{1,n} - \delta_{1,n-1}$
1	1.36175279e+01	– – –	1.11579415e+01	– – –
2	8.29844510e+00	-5.3e+00	7.57460662e+00	-3.6e+00
3	7.69807112e+00	-6.0e-01	6.97211386e+00	-6.0e-01
4	7.57782290e+00	-1.2e-01	6.83972864e+00	-1.3e-01
5	7.55390503e+00	-2.4e-02	6.81347460e+00	-2.6e-02
6	7.54857906e+00	-5.3e-03	6.80758174e+00	-5.9e-03
7	7.54747726e+00	-1.1e-03	6.80631795e+00	-1.3e-03
8	7.54724159e+00	-2.4e-04	6.80604419e+00	-2.7e-04
9	7.54719154e+00	-5.0e-05	6.80598601e+00	-5.8e-05
10	7.54718076e+00	-1.1e-05	6.80597353e+00	-1.2e-05
11	7.54717846e+00	-2.3e-06	6.80597086e+00	-2.7e-06

Table 7: Estimations of the value $\delta_{1,n} = \delta_{1,n}(\omega) = \boldsymbol{\delta} \frac{\widetilde{\alpha}_n(\omega_0)}{\widetilde{\alpha}_{n-1}(2\omega_0)}$ for $\omega_0 = \frac{\sqrt{5}-1}{2}$ on the left and $\omega_1 = 2\frac{\sqrt{5}-1}{2}$ on the right.

n	$\delta_{1,n}(\omega_0)$	$\delta_{1,n} - \delta_{1,n-1}$
1	9.52608610e+00	– – –
2	8.35338804e+00	-1.2e+00
3	8.23204689e+00	-1.2e-01
4	8.20385506e+00	-2.8e-02
5	8.19937833e+00	-4.5e-03
6	8.19817945e+00	-1.2e-03
7	8.19796400e+00	-2.2e-04
8	8.19791815e+00	-4.6e-05
9	8.19790879e+00	-9.4e-06
10	8.19790672e+00	-2.1e-06
11	8.19790628e+00	-4.4e-07

Table 8: Estimations of the value $\delta_{1,n} = \delta_{1,n}(\omega) = \boldsymbol{\delta} \frac{\widetilde{\alpha}_n(\omega_0)}{\widetilde{\alpha}_{n-1}(2\omega_0)}$ for the family (10) with $\omega_0 = \frac{\sqrt{5}-1}{2}$.

in the right through the affine map L given by (11). The value of δ_0 has been taken equal to the Feigenbaum constant and $\delta_1 \approx$ 7.54718 the experimental value obtained in Table 7. The results indicate that self-similarity properties extend to the whole reducibility region around each period doubling bifurcation.

4 Non-universality of the ratio sequence

A natural question to ask after the numerical evidences of universality and renormalization reported in the previous sections is "how general are these phenomena?". In this section we present an example which demonstrates that the universality and the self similarity properties depend on the Fourier expansion of the quasi-periodic forcing.

Consider the following family,

$$\left.\begin{aligned} \bar{\theta} &= \theta + \omega, \\ \bar{x} &= \alpha x(1 - x) + \varepsilon(\cos(2\pi\theta) + E\cos(4\pi\theta)). \end{aligned}\right\} \tag{12}$$

We consider E a fixed value and α and ε as true parameters, obtaining a two parametric family. We note that for $E = 0$ we recover the map (10).

n	$\widetilde{\alpha}_n(\omega)$	$\widetilde{\alpha}_n(\omega)/\widetilde{\alpha}_{n-1}(\omega)$	ϵ_a
0	-4.4000000000e+00	- - -	2.1e-14
1	-8.5708073961e+00	1.9479107718e+00	3.2e-14
2	-1.2367363641e+01	1.4429636637e+00	2.5e-12
3	-2.2002414361e+01	1.7790707058e+00	2.0e-14
4	-1.5466051366e+01	7.0292519321e-01	1.2e-13
5	-1.7124001858e+01	1.1071993396e+00	7.5e-13
6	-2.5233583736e+01	1.4735798293e+00	5.0e-11
7	-4.5526415150e+01	1.8041993411e+00	4.4e-12
8	-4.0793050977e+01	8.9603037802e-01	3.7e-12
9	-5.9579098646e+01	1.4605207804e+00	1.1e-09
10	-1.0695246126e+02	1.7951339260e+00	9.0e-11
11	-1.0464907069e+02	9.7846341692e-01	3.1e-09

Table 9: Approximate values of $\widetilde{\alpha}_n(\omega)$ of the family (12) for $\omega = \frac{\sqrt{5}-1}{2}$ and $E = 10^{-1}$.

We have done the computation of the values $\widetilde{\alpha}_n(\omega)$ for the family (12), for $E = 10^{-1}, 10^{-2}, 10^{-3}$ and $\omega = \frac{\sqrt{5}-1}{2}, 2\frac{\sqrt{5}-1}{2}$. The results are shown in Tables 9 to 14. To compute the values in the tables we have used the same procedure as for the families (7) and (10) before. In these tables we have also included the estimated values of the ratios $\widetilde{\alpha}_n(\omega)/\widetilde{\alpha}_{n-1}(\omega)$ and the estimated accuracies. In Table 15 we include the ratios $\delta_{1,n}(\omega) = \widetilde{\alpha}_n(\omega)/\widetilde{\alpha}_{n-1}(2\omega)$ and the differences $\delta_{1,n}(\omega) - \delta_{1,n-1}(\omega)$.

In the third column of Tables 9 to 14 we can observe that the relations given by (8) do not hold in this case. Moreover, if $f(\theta, x) = \alpha x(1-x)(1+\varepsilon \cos(2\pi\theta))$ and $g(\theta, x) = \alpha x(1-x) + \varepsilon(\cos(2\pi\theta) + E\cos(4\pi\theta))$, the numerical results displayed in these tables suggest that

$$\lim_{n\to\infty} \left[\frac{\widetilde{\alpha}_n(\omega, f)}{\widetilde{\alpha}_{n-1}(\omega, f)} - \frac{\widetilde{\alpha}_n(\omega, g)}{\widetilde{\alpha}_{n-1}(\omega, g)} \right] \neq 0.$$

We can also observe in Table 15 that the different sequences $\boldsymbol{\delta}\widetilde{\alpha}_n(\omega)/\widetilde{\alpha}_{n-1}(2\omega)$ cease to converge. Recall that the limit of this sequence gives the scale factor between the bifurcations diagrams of the map and of the square of the map. In other words, the self-similarity properties of the maps disappear.

Analyzing the results with more detail we can observe in Tables 9 to 15 that (when the parameter E is small) the map is not self-similar, but it behaves "close to self-similar" in the following sense: The values $\widetilde{\alpha}_n(\omega)$ for the family (10) that were shown in Table 5 become, for the family (12), the values shown in Tables 9, 11 and 13. Similarly, the values in Table 6 become, for $E \neq 0$, the values shown in Tables 10, 12 and 14. Note that the change in these values when $E \neq 0$ is of the order of E. This implies that the differences $\delta_{1,n} - \delta_{1,n-1}$ are also of the order of E.

5   Summary and conclusions

We have performed a numerical study of the asymptotic behaviour of the slopes $\widetilde{\alpha}_n(\omega, f)$ of the reducibility loss bifurcation curves of quasi-periodic perturbations of the Logistic Map. The results can be summarized as follows.

- **First numerical observation:** We have computed the sequences $\widetilde{\alpha}_n(\omega)/\widetilde{\alpha}_{n-1}(\omega)$ for the maps (7) and (10). They do not look convergent but the difference between these two

n	$\widetilde{\alpha}_n(\omega)$	$\widetilde{\alpha}_n(\omega)/\widetilde{\alpha}_{n-1}(\omega)$	ϵ_a
0	-4.4000000000e+00	- - -	4.2e-15
1	-6.8849393233e+00	1.5647589371e+00	2.6e-13
2	-1.2339134533e+01	1.7921921972e+00	1.9e-15
3	-8.8252833730e+00	7.1522709709e-01	1.0e-14
4	-9.9507316299e+00	1.1275254526e+00	2.6e-14
5	-1.5240261120e+01	1.5315719172e+00	4.9e-12
6	-2.6987715314e+01	1.7708171207e+00	6.9e-13
7	-2.4101506278e+01	8.9305471016e-01	1.0e-12
8	-3.4274713216e+01	1.4220983876e+00	1.4e-10
9	-5.9739968275e+01	1.7429750002e+00	4.0e-11
10	-6.0772668123e+01	1.0172865818e+00	3.5e-10
11	-9.7063373626e+01	1.5971550472e+00	8.3e-09

Table 10: Approximate values of $\widetilde{\alpha}_n(\omega)$ of the family (12) for $\omega = 2\frac{\sqrt{5}-1}{2}$ and $E = 10^{-1}$.

n	$\widetilde{\alpha}_n(\omega)$	$\widetilde{\alpha}_n(\omega)/\widetilde{\alpha}_{n-1}(\omega)$	ϵ_a
0	-4.0400000000e+00	- - -	2.6e-14
1	-8.1970065912e+00	2.0289620275e+00	4.9e-14
2	-1.1286613379e+01	1.3769189098e+00	2.4e-12
3	-2.1298993542e+01	1.8871022535e+00	2.1e-14
4	-1.4654396022e+01	6.8803232383e-01	8.9e-14
5	-1.5964802815e+01	1.0894207302e+00	5.0e-13
6	-2.3545880397e+01	1.4748619617e+00	4.5e-11
7	-4.4967877741e+01	1.9097981041e+00	5.6e-12
8	-3.8501241787e+01	8.5619432630e-01	4.8e-12
9	-5.4345411904e+01	1.4115236128e+00	1.1e-09
10	-1.0260055779e+02	1.8879341272e+00	1.0e-10
11	-9.7178352178e+01	9.4715227943e-01	2.3e-09

Table 11: Approximate values of $\widetilde{\alpha}_n(\omega)$ of the family (12) for $\omega = \frac{\sqrt{5}-1}{2}$ and $E = 10^{-2}$.

n	$\widetilde{\alpha}_n(\omega)$	$\widetilde{\alpha}_n(\omega)/\widetilde{\alpha}_{n-1}(\omega)$	ϵ_a
0	-4.0400000000e+00	- - -	3.8e-15
1	-6.2967793362e+00	1.5586087466e+00	2.4e-13
2	-1.2062745707e+01	1.9157008786e+00	2.1e-15
3	-8.3390918858e+00	6.9130959805e-01	9.0e-15
4	-9.1092083960e+00	1.0923501648e+00	4.6e-14
5	-1.3509885744e+01	1.4831020608e+00	4.7e-12
6	-2.5722289496e+01	1.9039605503e+00	6.1e-13
7	-2.2023032848e+01	8.5618478288e-01	6.8e-13
8	-3.0953588852e+01	1.4055098163e+00	1.2e-10
9	-5.8281365651e+01	1.8828629510e+00	5.1e-11
10	-5.5448581611e+01	9.5139468666e-01	2.5e-10
11	-8.6313143445e+01	1.5566339289e+00	8.2e-09

Table 12: Approximate values of $\widetilde{\alpha}_n(\omega)$ of the family (12) for $\omega = 2\frac{\sqrt{5}-1}{2}$ and $E = 10^{-2}$.

n	$\widetilde{\alpha}_n(\omega)$	$\widetilde{\alpha}_n(\omega)/\widetilde{\alpha}_{n-1}(\omega)$	ϵ_a
0	-4.0040000000e+00	- - -	2.7e-14
1	-8.1643491058e+00	2.0390482282e+00	5.0e-14
2	-1.1178647202e+01	1.3692024995e+00	2.4e-12
3	-2.1229290655e+01	1.8990930004e+00	2.1e-14
4	-1.4573231305e+01	6.8646812284e-01	8.6e-14
5	-1.5850170411e+01	1.0876222355e+00	4.7e-13
6	-2.3400073191e+01	1.4763294391e+00	4.5e-11
7	-4.4929300750e+01	1.9200495820e+00	5.7e-12
8	-3.8285483755e+01	8.5212730036e-01	5.8e-12
9	-5.3822109356e+01	1.4058098286e+00	1.1e-09
10	-1.0217709608e+02	1.8984223641e+00	1.0e-10
11	-9.6437862923e+01	9.4383053171e-01	2.2e-09

Table 13: Approximate values of $\widetilde{\alpha}_n(\omega)$ of the family (12) for $\omega = \frac{\sqrt{5}-1}{2}$ and $E = 10^{-3}$.

n	$\widetilde{\alpha}_n(\omega)$	$\widetilde{\alpha}_n(\omega)/\widetilde{\alpha}_{n-1}(\omega)$	ϵ_a
0	-4.0040000000e+00	- - -	3.7e-15
1	-6.2470810635e+00	1.5602100558e+00	2.4e-13
2	-1.2039370639e+01	1.9271993618e+00	2.1e-15
3	-8.2941266770e+00	6.8891696467e-01	9.0e-15
4	-9.0277699390e+00	1.0884533466e+00	4.8e-14
5	-1.3337423899e+01	1.4773774686e+00	4.7e-12
6	-2.5600860673e+01	1.9194756698e+00	6.1e-13
7	-2.1815381589e+01	8.5213469453e-01	6.3e-13
8	-3.0654499563e+01	1.4051782426e+00	1.2e-10
9	-5.8180013759e+01	1.8979273708e+00	5.2e-11
10	-5.4936892373e+01	9.4425712239e-01	2.4e-10
11	-8.5250385421e+01	1.5517875464e+00	8.2e-09

Table 14: Approximate values of $\widetilde{\alpha}_n(\omega)$ of the family (12) for $\omega = 2\frac{\sqrt{5}-1}{2}$ and $E = 10^{-3}$.

n	$\delta_{1,n}(\omega)$	$\delta_{1,n} - \delta_{1,n-1}$	n	$\delta_{1,n}(\omega)$	$\delta_{1,n} - \delta_{1,n-1}$	n	$\delta_{1,n}(\omega)$	$\delta_{1,n} - \delta_{1,n-1}$
1	9.095188	- - -	1	9.473633	- - -	1	9.520727	- - -
2	8.387251	-7.1e-01	2	8.369274	-1.1e+00	2	8.355159	-1.2e+00
3	8.325844	-6.1e-02	3	8.244333	-1.2e-01	3	8.233307	-1.2e-01
4	8.182639	-1.4e-01	4	8.205249	-3.9e-02	4	8.204041	-2.9e-02
5	8.035129	-1.5e-01	5	8.183245	-2.2e-02	5	8.197777	-6.3e-03
6	7.730884	-3.0e-01	6	8.137779	-4.5e-02	6	8.191961	-5.8e-03
7	7.876621	1.5e-01	7	8.162729	2.5e-02	7	8.194411	2.4e-03
8	7.902866	2.6e-02	8	8.162820	9.1e-05	8	8.194339	-7.1e-05
9	8.116387	2.1e-01	9	8.197747	3.5e-02	9	8.198023	3.7e-03
10	8.359271	2.4e-01	10	8.219826	2.2e-02	10	8.200161	2.1e-03
11	8.040253	-3.2e-01	11	8.183173	-3.7e-02	11	8.196456	-3.7e-03

Table 15: Estimations of the value $\delta_{1,n} = \delta_{1,n}(\omega) = \boldsymbol{\delta}\frac{\widetilde{\alpha}_n(\omega)}{\widetilde{\alpha}_{n-1}(2\omega)}$ for the map (12) (where $\boldsymbol{\delta}$ is the Feigenbaum constant). The different boxes correspond (from left to right) to $E = 10^{-1}, 10^{-2}$ and 10^{-3}. In all the cases we have taken $\omega = \frac{\sqrt{5}-1}{2}$.

sequences seems to have zero limit.

- **Second numerical observation:** The sequence $\widetilde{\alpha}_n(\omega)/\widetilde{\alpha}_{n-1}(2\omega)$ seems to be convergent in n. The limit depends on ω and on the particular family considered.

- **Third numerical observation:** The two previous observations are not true for the map (12). The sequence seems to be E-close to the corresponding sequence for $E = 0$ (i.e., map (10)).

These numerical observations evidence the existence of some structure governing the asymptotic behaviour of the sequence $\widetilde{\alpha}_n(\omega)$. In a sequence of forthcoming papers ([17, 18, 19]) we will study the renormalization operator for these maps to give an explanation of these phenomena.

References

[1] L. Alsedà and S. Costa, On the definition of strange nonchaotic attractor, *Fund. Math.*, 206:23–39, 2009.

[2] D.H. Bailey, Y. Hida, X.S. Li, and Y. Renard. http://crd.lbl.gov/ dhbailey/mpdist/.

[3] K. Bjerklöv. SNA's in the quasi-periodic quadratic family. *Comm. Math. Phys.*, 286(1):137–161, 2009.

[4] E. Castellà and A. Jorba. On the vertical families of two-dimensional tori near the triangular points of the bicircular problem. *Celestial Mech. Dynam. Astronom.*, 76(1):35–54, 2000.

[5] W. de Melo and S. van Strien. *One-dimensional dynamics*, volume 25 of *Ergebnisse der Mathematik und ihrer Grenzgebiete (3) [Results in Mathematics and Related Areas (3)]*. Springer-Verlag, Berlin, 1993.

[6] U. Feudel, S. Kuznetsov, and A. Pikovsky. *Strange nonchaotic attractors*, volume 56 of *World Scientific Series on Nonlinear Science. Series A: Monographs and Treatises*. World Scientific Publishing Co. Pte. Ltd., Hackensack, NJ, 2006. Dynamics between order and chaos in quasiperiodically forced systems.

[7] J. Figueras and A. Haro. Reliable computation of robust response tori on the verge of breakdown *SIAM J. Appl. Dyn. Syst.* (to appear).

[8] C. Grebogi, E. Ott, Pelikan S., and J.A. Yorke. Strange attractors that are not chaotic. *Phys. D*, 13(1-2):261–268, 1984.

[9] J. F. Heagy and S. M. Hammel. The birth of strange nonchaotic attractors. *Phys. D*, 70(1-2):140–153, 1994.

[10] T. H. Jaeger. Quasiperiodically forced interval maps with negative schwarzian derivative. *Nonlinearity*, 16(4):1239–1255, 2003.

[11] A. Jorba. Numerical computation of the normal behaviour of invariant curves of n-dimensional maps. *Nonlinearity*, 14(5):943–976, 2001.

[12] A. Jorba, P. Rabassa, and J.C. Tatjer. Period doubling and reducibility in the quasi-periodically forced logistic map. *Discrete Contin. Dyn. Syst. Ser. B*, 17(5):1507–1535, 2012.

[13] A. Jorba and J. C. Tatjer. A mechanism for the fractalization of invariant curves in quasi-periodically forced 1-D maps. *Discrete Contin. Dyn. Syst. Ser. B*, 10(2-3):537–567, 2008.

[14] K. Kaneko. Doubling of torus. *Progr. Theoret. Phys.*, 69(6):1806–1810, 1983.

[15] A. Prasad, V. Mehra, and R. Ramaskrishna. Strange nonchaotic attractors in the quasiperiodically forced logistic map. *Phys. Rev. E*, 57(2):1576–1584, 1998.

[16] P. Rabassa. *Contribution to the study of perturbations of low dimensional maps.* PhD thesis, Universitat de Barcelona, 2010.

[17] P. Rabassa, A. Jorba, and J.C. Tatjer. Towards a renormalization theory for quasi-periodically forced one dimensional maps I. Existence of reducibily loss bifurcations. In preparation, 2012.

[18] P. Rabassa, A. Jorba, and J.C. Tatjer. Towards a renormalization theory for quasi-periodically forced one dimensional maps II. Asymptotic behaviour of reducibility loss bifurcations. In preparation, 2012.

[19] P. Rabassa, A. Jorba, and J.C. Tatjer. Towards a renormalization theory for quasi-periodically forced one dimensional maps III. Numerical support. In preparation, 2012.